

Effects of drop size and measuring condition on static contact angle measurement on a superhydrophobic surface with goniometric technique

Kwangseok Seo*, Minyoung Kim*, Jeong Keun Ahn**, and Do Hyun Kim*[†]

*Department of Chemical and Biomolecular Engineering, Korea Advanced Institute of Science and Technology, Daejeon 305-701, Korea

**Department of Microbiology, Chungnam National University, Daejeon 305-764, Korea

(Received 3 November 2014 • accepted 9 February 2015)

Abstract—It is not a simple task to measure a contact angle of a water drop on a superhydrophobic surface with sessile drop method, because a roll-off angle is very low. Usually contact angle of a water drop on a superhydrophobic surface is measured by fixing a drop with intentional defects on the surface or a needle. We examined the effects of drop size and measuring condition such as the use of a needle or defects on the static contact angle measurement on superhydrophobic surface. Results showed that the contact angles on a superhydrophobic surface remain almost constant within intrinsic measurement errors unless there is a wetting transition during the measurement. We expect that this study will provide a deeper understanding on the nature of the contact angle and convenient measurement of the contact angle on the superhydrophobic surface.

Keywords: Superhydrophobic Surface, Sessile Drop Method, Goniometric Technique, Contact Angle, Water Drop

INTRODUCTION

A superhydrophobic surface exhibits a very high water contact angle greater than 150° and a very low water drop roll-off angle less than 10° [1]. Because a superhydrophobic surface has extreme water repellency originating from the immensely small area of the solid surface actually contacting with water, there have been various researches on the applications of these unique features. Various applications, such as self-cleaning effect [2], drag-reduction [3-5], a stain-free fabric [6,7], water-oil collecting system [8-11], and droplet guiding system [12,13], have been studied by applying a superhydrophobic surface.

For superhydrophobicity, a surface should have a low surface energy and highly roughened topography [14]. Various fabrication methods have been reported, such as laser ablation [15,16], solvent/non-solvent phase separation [17], CVD [18], metal etching [19], electroless galvanic deposition [20], sol-gel processing [21,22], polymer templating [23].

Water contact angle on the superhydrophobic surface is usually measured to determine the wettability. The most widely used method is to measure the contact angle of a sessile drop resting on the superhydrophobic surface. But placing the drop on the superhydrophobic surface is not easy, because a superhydrophobic surface has a very low roll-off angle. Even with a slight vibration, the water drop

placed on the surface easily rolls off. Especially, in the case of a drop of small size on the superhydrophobic surface with roll-off angle close to zero, it is almost impossible to measure the contact angle with the sessile drop method. In some previous works involving the measurement of a contact angle on the superhydrophobic surface, a water drop is generated from a needle tip of a syringe to the surface and the contact angle is measured [24-27]. In some cases small defects have been used to pin the drop on superhydrophobic surface [28]. However, there have been few studies on how much these factors affect a contact angle.

In this study, to measure the contact angle of the water drop on superhydrophobic surface, some measuring methods will be discussed from theoretical consideration on the meaning of a contact angle.

SUPERHYDROPHOBIC SURFACE AS PSEUDO-IDEAL SURFACE

From a thermodynamic point of view, the contact angle of a drop on an ideal surface is a necessary condition that must be satisfied at the contact line in order to minimize the total energy of the system. This can be understood more clearly from the energy minimization approach [29,30].

An optimal contact angle (the most stable angle in the system) must be satisfied at the contact line in order to minimize the total energy of the system. In other words, unless the optimal contact angle is met at the contact line, the system cannot be at the lowest energy state and residual force exists at the contact line. If the contact line moves freely on the surface, the contact line will move to satisfy the optimal contact angle, changing the shape of the drop [30]. From the condition at the contact line, Young's equation, Cas-

[†]To whom correspondence should be addressed.

E-mail: dohyun.kim@kaist.ac.kr

^{*}This paper is dedicated to Professor Hwayong Kim to celebrate his retirement from the School of chemical and biological engineering of Seoul National University.

Copyright by The Korean Institute of Chemical Engineers.

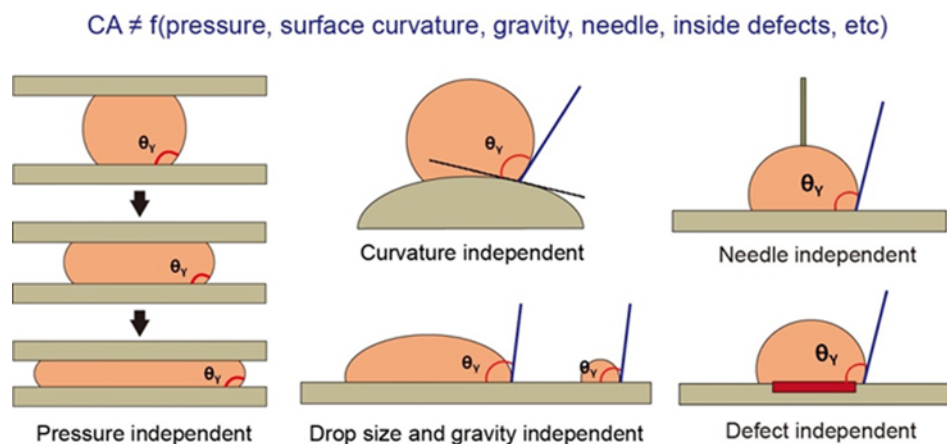


Fig. 1. Theoretically, a contact angle is not a function of pressure, surface curvature, existence of a needle, drop size, gravity, and a defect inside contact line. CA means contact angle.

sie-Baxter equation and Wenzel equation can be derived.

There are two important facts deducible from the thermodynamic approaches. Firstly, the contact angle is determined only at the local region near contact line. For example, the property of internal surface under the drop does not affect the contact angle. Secondly, contact angle is independent of the external factors not related to the surface energy. In an ideal situation, as shown in Fig. 1, contact angle is not affected by pressure, drop size, gravity, surface curvature, and existence of a needle or defects.

It should be noted that the contact line has been assumed to move freely on the surface for the ideal situation. This assumption does not describe the actual situation on the real common surface. Because the real surface has contact angle hysteresis, the contact line cannot move freely on the surface. In addition, the static contact angle has some values between two extremal values, i.e. a receding angle and an advancing angle. So, it is hard to describe the actual surface with a single equation such as Wenzel equation or Cassie-Baxter equation. However, because superhydrophobic surface has a very low contact angle hysteresis, the contact line can easily move on the superhydrophobic surface and the surface has a narrow range of static contact angles. We believe that this is why Cassie-Baxter equation and Wenzel equation have been widely used for the superhydrophobic surface.

Table 1 compares wetting properties of three types of surfaces (common surface, ideal surface, superhydrophobic surface). In the table, superhydrophobic surface seem to have similar wetting properties with ideal surface except a high contact angle. In this study, we consider superhydrophobic surface as pseudo-ideal surface in that the contact line can easily move. With the above facts, effects of drop size, existence of a needle, and a defect on static contact angles on the superhydrophobic surface will be discussed.

Table 1. Comparison of wetting properties of three types of surfaces

	Common surface	Ideal surface	Superhydrophobic surface
Contact angle	Less than 120°	From 0° to 180°	Higher than 150°
Contact angle hysteresis	High or medium	Zero	Very low
Movement of contact line	Difficult	Always possible	Very easy

EXPERIMENTAL

1. Fabrication of a Superhydrophobic Surface

Methyltrichlorosilane ($\geq 97\%$, Sigma-Aldrich) and toluene (Extra Pure, ASSAY (GC) min 99%, Junsei) were used for the superhydrophobic coating. The superhydrophobic coating was applied employing the procedure by Gao et al. [31].

They made a perfect ultraphobic surface and verified it from compression and release test of a water drop. The surface had no affinity for water and there was no wetting transition during the test. We selected this surface as a sample surface for the experiment. However, their surface has a very high contact angle (advancing angle/receding angle = $180^\circ/180^\circ$). High contact angle of this degree cannot be accurately measured with the sessile drop method [31], because small variation in locating the triple line causes large errors in measurement of the contact angle [32]. Thus, for the surface with lower contact angle, we used toluene, instead of anhydrous toluene which they used [31].

First, a glass slide was ultrasonically cleaned with deionized water and ethanol. After drying in a clean oven at 120 °C for 15 min, the glass slide was placed in a glass petri dish and covered with 1.0 M methyltrichlorosilane solution in toluene. The petri dish was closed with the cover. The reaction time depends on relative humidity. For a uniform film, it took about 1 day (about relative humidity = 60%). After reaction, the glass slide was repeatedly rinsed with toluene, ethanol, ethanol-water (1:1), and water in this order and dried in a clean container at room temperature.

2. Drop Deposition Method

2-1. Drop Size Effect

The superhydrophobic coating was placed on a stage of the contact angle analyzer. Water drops of various sizes were gently dropped

on the superhydrophobic coating with pipette. When dropping a water drop, the drop rolled-off anywhere but finally came to a stop. The drop was moved to the desired position for the recording with camera by slowly moving the stage.

2-2. Defect Effect

Defects were made by scraping the superhydrophobic coating with a sharp scalpel. The defect size was about 0.7 mm. Initially, a water drop of 1 μL was carefully placed on the defect. After the contact angle was measured, water was continuously added up for larger drops.

2-3. Needle Effect

A syringe with a flat needle (diameter: 0.41 mm) was installed with the contact angle analyzer. A water drop with the desired volume was placed on the superhydrophobic coating with pipette. A trace of water was ejected from the needle and gently touched with the water drop on the coating by moving up the stage.

2-4. Drop Distortion Effect

A water drop of 10 μL was ejected from the needle and gently touched with the superhydrophobic coating. The stage was vertically moved to control the distance between the tip of the needle and the coating for perturbation in the shape of the drop.

3. Characterization

The morphology and microstructure of the superhydrophobic coating have been investigated using field emission scanning electron microscope (FE-SEM, Nova 230, FEI).

Contact angles (static, advancing, and receding angles) were analyzed with contact angle analyzer (Phoenix 300, SEO). Images of the contact angles were magnified and all the contact angles were measured with manual mode because the software of the contact angle analyzer could not automatically catch exact base lines of water drops of various sizes.

Even in the case of the same drops, there are some fluctuations of contact angles in measuring the static contact angles due to air convection, setting of camera angle and back lighting, and setting of a baseline of a drop. The intrinsic error of the measurement method has been known as about 2° [33]. The images of the contact angles were selected as images with contact angles corresponding to each average value of contact angles for measurement more than minimum six times.

RESULTS AND DISCUSSION

1. Surface Analysis

It was verified from SEM image that the superhydrophobic coat-

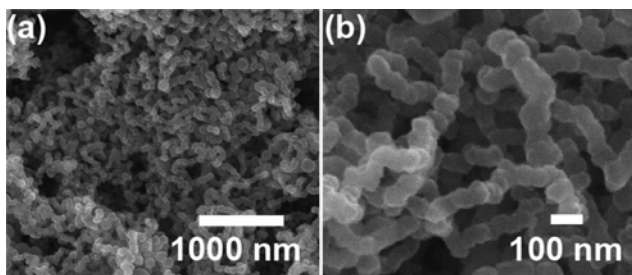


Fig. 2. SEM image of the superhydrophobic coating.

ing satisfied the condition that the surface must be highly roughened for superhydrophobicity. As shown in Fig. 2, very small spherical particles of tens of nanometer in size generated during polymerization were coagulated and formed an interconnected network. It is observed that the size and structure of these are irregular. These irregular agglomerates increase the total roughness of the surface. Due to an increase in surface roughness by formation of non-uniform aggregates with intrinsic hydrophobicity of the network (methylsilicone) [31], the coating could have superhydrophobicity. The advancing angle and receding angle of the coating were about $169^\circ \pm 2^\circ$ and $163^\circ \pm 2^\circ$, respectively. The roll-off angles of a water drop (10 μL) were less than 1° . The coating had low contact angle hysteresis of about 6° . It indicates that water drops is in the Cassie wetting regime where the micro/nano-sized gaps are formed between liquid and solid and anti-adhesive property is achieved.

As to the robustness of a superhydrophobic surface, irreversible wetting transition can be induced between Cassie state to Wenzel state by external pressure [34] or condensation [35]. It can significantly affect a contact angle and contact angle hysteresis [36]. However, there was no wetting transition during the experiment. The surface always had little affinity for water. For robust superhydrophobic surface against the transition, large surface roughness is required [36]. The superhydrophobic surface used in the experiment could avoid the wetting transition due to large surface roughness, as shown in Fig. 2. Thus, the superhydrophobic surface was robust against the transition.

2. Effect of Drop Size, Defect, Needle and Drop Distortion on Contact Angle

Fig. 3 shows the contact angle behavior on water drops of various sizes. As mentioned earlier, the size of a water drop is not a

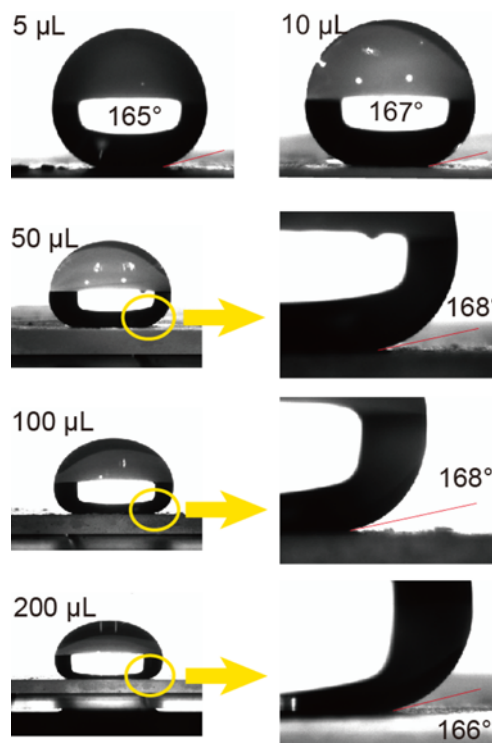


Fig. 3. Contact angle behavior of water drops of various size.

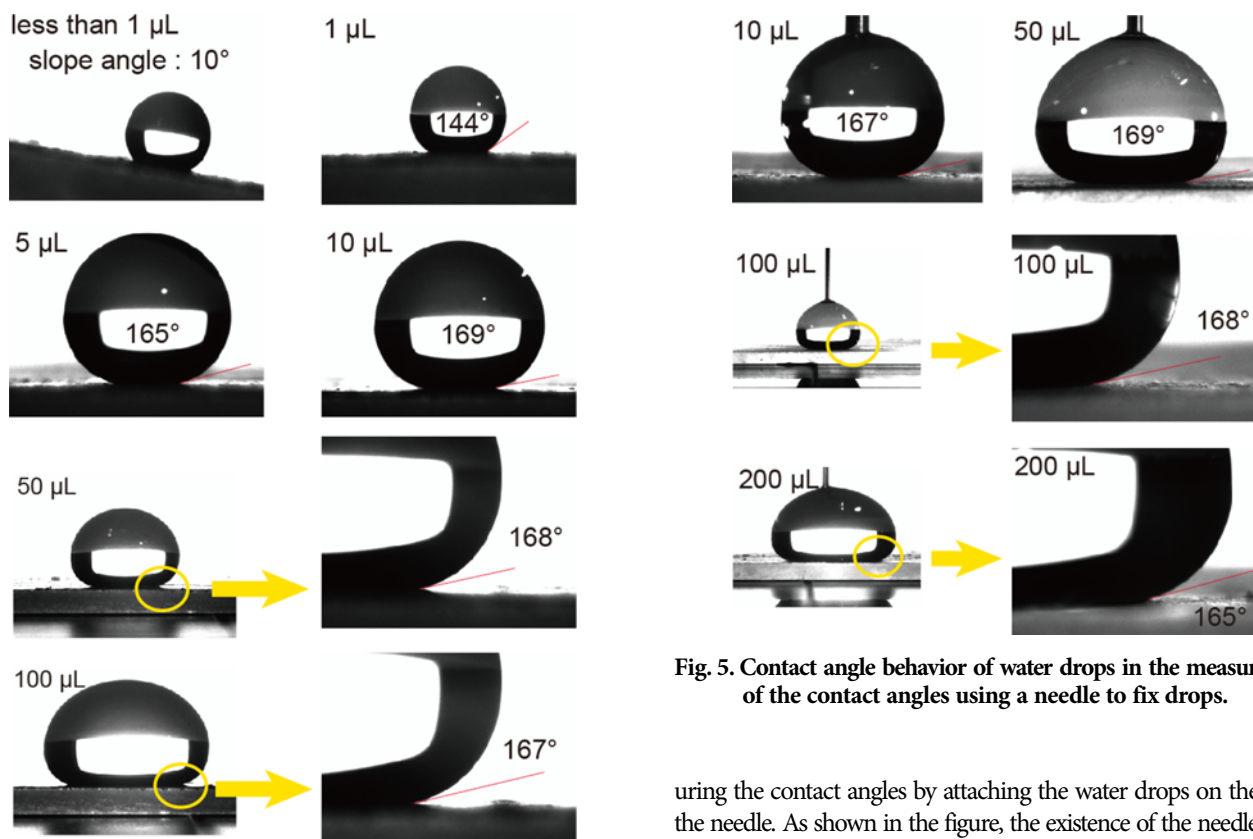


Fig. 4. Contact angle behavior of water drops on an intentional defect.

factor that affects the contact angle in the contact line. Therefore, regardless of the size of the drop, the contact angle should be always the same. Although a droplet grows gradually from the sphere form to the puddle form with the increasing volume, the contact angles are almost the same within inherent errors of the measurement method.

Fig. 4 shows the contact angle behavior of water drops on an intentional defect. The water drop pinned by the defect did not roll off on the coating with a considerable inclination (10°). The size of the defect was about 0.7 mm. In the case of the water drop of $1\ \mu\text{L}$, the contact line was located within the defect. At this time, the contact angle increases with an increase of the drop volume. Above a certain value of the drop volume, this contact line is placed outside the defect and the contact angles remain almost the same, as shown in the figure.

Fig. 5 shows contact angle behavior of water drops when meas-

Fig. 5. Contact angle behavior of water drops in the measurement of the contact angles using a needle to fix drops.

uring the contact angles by attaching the water drops on the tip of the needle. As shown in the figure, the existence of the needle rarely affects the contact angles. In other words, although the shape of the upper part of the drop was changed by the existence of the needle, it did not affect the contact angle near contact line. This is because theoretically, the shape deformation of the drop cannot affect contact angles in an ideal situation.

When contact angles are measured with a needle, the shape of a drop will be distorted by a needle, depending on a distance between the coating and the tip of needle. Fig. 6 shows contact angle behavior on the distortion of a drop by a needle. The shape of the drop was distorted depending on the distance between the coating and the needle. The pressure in the drop was also changed. As shown, the distortion of the drop did not have a significant impact on the contact angle. Because it is easy for the contact line to move on the superhydrophobic surface, the change of the distance transfers the position of the contact line while the contact angle remains almost same. Actually, it can be verified that the length of the baseline changed depending on the distance.

It is somewhat tiresome to apply the sessile drop method to superhydrophobic surface because of difficulties in the placement of a water drop on the surface. However, a contact angle can be easily

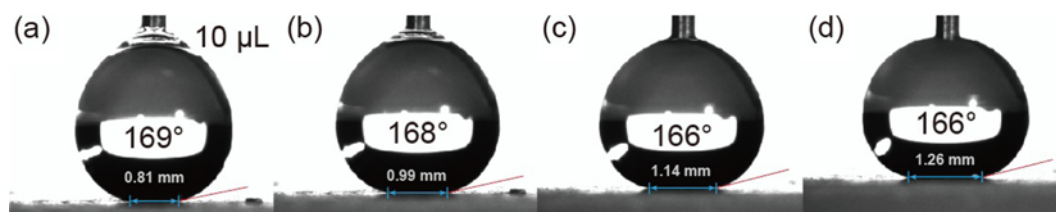


Fig. 6. Contact angle behavior on the distortion of a drop.

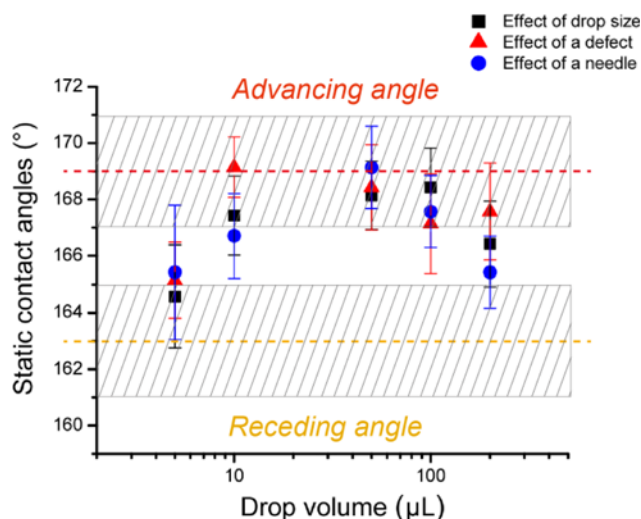


Fig. 7. The effect of drop size, existence of defects and use of a needle on static contact angles.

measured on a superhydrophobic surface by pinning the drop on an artificial defect or attaching it on a needle tip. The contact angle obtained from these methods has no significant difference from the values obtained by the sessile drop in intrinsic measurement errors, when no wetting transition occurs. On a superhydrophobic surface, it can be concluded that these factors, such as drop size, defects inside contact line, and the use of a needle tip, do not affect the contact angle enough to exceed the extrema of contact angle of the surface, i.e., an advancing angle and a receding angle (Fig. 7). However, these factors can greatly affect the contact angle on general surface with large contact angle hysteresis.

In practice, there is a little deviation between static contact angles, as shown in Fig. 7. However, it is impossible to distinguish whether the deviation is caused by these factors or experimental errors from the results. To examine whether these effects actually affect a contact angle, more sensitive measurement method with smaller intrinsic errors should be considered [32]. Nevertheless, they are negligible because the extent of the impact is within the intrinsic error of the measurement method, when contact angle hysteresis of superhydrophobic surface is comparable to the error. We expect that these results will provide convenient measurement of a contact angle on a superhydrophobic surface.

CONCLUSION

Effects of drop size, existence of defects or a needle in measuring the static contact angles on superhydrophobic surface have been discussed. These effects do not affect the contact angle on the superhydrophobic surface, unless there is wetting transition in measuring the contact angle. This can be explained by the fact that a superhydrophobic surface is a pseudo-ideal surface in that the contact line can easily move and has a low contact angle hysteresis comparable to the intrinsic measurement error. We expect that the results will eliminate a suspicion about the simple contact angle measurement on the superhydrophobic surface and provide deeper understanding on the meaning of contact angle.

ACKNOWLEDGEMENT

This work was supported by the National Research Foundation of Korea (NRF) grant funded by the Korea government (MSIP) (No. 2012R1A2A2A01047371).

REFERENCES

1. C. Dorrer and J. R uhe, *Soft Matter*, **5**, 51 (2009).
2. K. M. Wisdom, *PNAS*, **110**, 7992 (2013).
3. B. Bhushan, *Beilstein J. Nanotechnol.*, **2** 66 (2011).
4. H. Dong, M. Cheng, Y. Zhang, H. Wei and F. Shi, *J. Mater. Chem. A*, **1**, 5886 (2013).
5. N. J. Shirtcliffe, G. McHale, M. I. Newton and Y. Zhang, *ACS Appl. Mater. Int.*, **1**, 1316 (2009).
6. Y. Zhao, Z. Xu, X. Wang and T. Lin, *Langmuir*, **28**, 6328 (2012).
7. B. Leng, Z. Shao, G. de With and W. Ming, *Langmuir*, **25**, 2456 (2009).
8. L. Feng, Z. Zhang, Z. Mai, Y. Ma, B. Liu, L. Jiang and D. Zhu, *Angew. Chem.*, **116**, 25 (2004).
9. C. Wang, T. Yao, J. Wu, C. Ma, Z. Fan, Z. Wang, Y. Cheng, Q. Lin and B. Yang, *ACS Appl. Mater. Int.*, **1**, 2613 (2009).
10. A. K. Kota, G. Kwon, W. Choi, J. M. Mabry and A. Tuteja, *Nat. Commun.*, **3**, 1025 (2012).
11. K. Seo, M. Kim and D. H. Kim, *Carbon*, **69**, 583 (2014).
12. H. Mertaniemi, V. Jokinen, L. Sainiemi, S. Franssila, A. Marmur, O. Ikkala and R. H. A. Ras, *Adv. Mater.*, **23**, 2911 (2011).
13. K. S. Seo, R. Wi, S. G. Im and D. H. Kim, *Polymer Adv. Tech.*, **24**, 1075 (2013).
14. M. Nosonovsky, *Langmuir*, **23**, 3157 (2007).
15. J. Noh, J.-H. Lee, S. Na, H. Li and D. H. Jung, *Jpn. J. Appl. Phys.*, **49**, 106502 (2010).
16. J. Bekesi, J. J. Kaakkunen, W. Michaeli, F. Klaiber, M. Schoengart, J. Ihlemann and P. Simon, *Appl. Phys. A*, **99**, 691 (2010).
17. H. Y. Erbil, A. L. Demirel, Y. Avci and O. Mert, *Science*, **299**, 1377 (2003).
18. R. Su, H. Liu, T. Kong, Q. Song, N. Li, G. Jin and G. Cheng, *Langmuir*, **27**, 13220 (2011).
19. H. Meng, S. Wang, J. Xi, Z. Tang and L. Jiang, *J. Phys. Chem. C*, **112**, 11454 (2008).
20. I. A. Larmour, S. E. J. Bell and G. C. Saunders, *Angew. Chem. Int.*, **46**, 1710 (2007).
21. Q. F. Xu, J. N. Wang and K. D. Sanderson, *ACS Nano*, **4**, 2201 (2010).
22. R. V. Lakshmi, T. Bharathidasan and B. J. Basu, *Appl. Surf. Sci.*, **257**, 10421 (2011).
23. Q. F. Xu, B. Mondal and A. M. Lyons, *ACS Appl. Mater. Inter.*, **3**, 3508 (2011).
24. X. Deng, L. Mannen, H.-J. Butt and D. Vollmer, *Science*, **335**, 67 (2012).
25. L.-D. Liu, C.-S. Lin, M. Tikekar and P.-H. Chen, *Thin Solid Films*, **519**, 6224 (2011).
26. D. K. Sarkar, *Surf. Coat. Technol.*, **204**, 2483 (2010).
27. K. Askar, B. M. Phillips, Y. Fang, B. Choi, N. Gozubenli, P. Jiang and B. Jiang, *Colloids Surf., A*, **439**, 84 (2013).
28. C. W. Extrand and S. I. Moon, *Langmuir*, **26**, 17090 (2010).
29. E. Bormashenko, *Langmuir*, **25**, 10451 (2009).

30. K. Seo, M. Kim and D. H. Kim, *Korea-Aust. Rheol. J.*, **25**, 175 (2013).
31. L. Gao and T. J. McCarthy, *J. Am. Chem. Soc.*, **128**, 9052 (2006).
32. S. Srinivasan, G. H. McKinley and R. E. Cohen, *Langmuir*, **27**, 13582 (2011).
33. A. S. Dimitrov, P. A. Kralchevsky, A. D. Nikolov, H. Noshi and M. Matsumoto, *J. Colloid Interface Sci.*, **145**, 279 (1991).
34. M. Reyssat, J. M. Yeomans and D. Quéré, *Europhys. Lett.*, **81**, 26006 (2008).
35. D. Lafuma and D. Quéré, *Nat. Mater.*, **2**, 457 (2003).
36. M. Callies and D. Quéré, *Soft Matter*, **1**, 55 (2005).